A Method for Simultaneous Computation of Bed and Bank Deformation of a River

Y. Shimizu
Hokkaido University, Hokkaido, Japan

ABSTRACT: A numerical model is developed to simulate the formation of braided stream, in which bank erosion and bed deformation are calculated simultaneously. Flow field, bed deformation, bank erosion and channel geometry are calculated numerically with a general coordinate system, which can be applied to any shape of channel geometry during the deformation of channel geometry due to the bank erosion. CIP method (Cubic Interpolated Pseudo-particle Method) is used to evaluate calculation results with high accuracy. Calculation is started with a narrow straight channel with flat bed, and in tern the development of alternate bar, channel meandering, appearance of mid channel bar, and finally, a braided channel geometry is simulated. Computational results are compared with experimental results and the applicability of the model is discussed.

1 INTRODUCTION

Determining the erosion of riverbeds and riverbanks quantitatively is important subject in disaster prevention works. The riverbed erosion in a fixed bank (experimental flumes, rivers with bank protection works, etc.) have been studied on theoretical and experimental basis and numerical models have been developed. As a result, the mechanism of river bed forms has been explained, and numerical models are being established (Shimizu et al. 1995). Studies on bank erosion and river meandering are also being made theoretically and experimentally from various viewpoints, making it possible to understand these events to some extent(Hasegawa & Ito 1978, Parker 1983).

The changes in the bed topography and the erosion of banks are not events that occur independently; both of them take place interdependently through water flow and sediment. In order to evaluate such events, particularly for natural rivers, where banks are not protected, a model is required that can deal with riverbed evolution and bank erosion simultaneously. From this point of view, this study aimed to develop such a model. As a first step towards this aim, this paper describes the development of a model for a river channel whose bed and banks consist of sandy soil. The basis of the model was the computation of a two-dimensional flow and the bed deformation. In order to make these computations, general coordinates, enabling a description of a boundary shape that takes an arbitrary form, is used assuming that erosion and sediment deposition occur in the cross-sectional direction to transform the plane shape of the water channel into an arbitrary shape. Flow field is calculated using a high-order Godunov scheme referred to as the CIP method (Yabe & Ishikawa 1990). It is assumed that the erosion of banks occurs when the gradient in the cross-sectional direction of the banks is steeper than the submerged angle of repose, because of changes in the riverbed erosion near the banks. In this case, the amount of sediment beyond the submerged critical angle of slope is included in the computation of the bankbed evolution, as a supply of sediment from the banks. On the other hand, the inner banks at channel bends and other parts, which are transformed into land, are successively excluded from the range of computation.

The computational model is verified by physical model experiment conducted by Bertoldi *et al.*(2001). The experimental results show that the model was effective in simulating precisely the erosion of banks and the changes in the

riverbed, i.e. the changes in free meandering and formation of bars through time. The model also proved to be able to quantitatively analyze the formation of multi-row bar channel or braided channel as well.

2 BASIC EQUATIONS OF FLOW

A moving boundary fitted coordinate (MBFC) system is employed for the flow and bed deformation in the domain where the channel width changes with time. Flow equations in co-orthogonal coordinates are given as follows.

$$\frac{\partial h}{\partial t}+\frac{\partial (hu)}{\partial x}+\frac{\partial (hv)}{\partial y}=0 \tag{1}$$

$$\frac{\partial (hu)}{\partial t}+\frac{\partial (hu^2)}{\partial x}+\frac{\partial (huv)}{\partial y}=-gh\frac{\partial H}{\partial x} - C_d u\sqrt{u^2+v^2}+h\nu_t\left(\frac{\partial^2 u}{\partial x^2}+\frac{\partial^2 u}{\partial y^2}\right) \tag{2}$$

$$\frac{\partial (hv)}{\partial t}+\frac{\partial (huv)}{\partial x}+\frac{\partial (hv^2)}{\partial y}=-gh\frac{\partial H}{\partial y} - C_d v\sqrt{u^2+v^2}+h\nu_t\left(\frac{\partial^2 v}{\partial x^2}+\frac{\partial^2 v}{\partial y^2}\right) \tag{3}$$

where x and y are co-orthogonal coordinates, t is time, u and v are depth averaged velocity components in x- and y- directions, respectively, h is depth, H is water surface elevation, g is acceleration of gravity, and C_d is bed friction coefficient.

Above equations in (x, y, t) coordinate system are transformed into MBFC system in (ξ, η, τ) coordinates using the following relations:

$$\begin{cases} \dfrac{\partial}{\partial t}=\dfrac{\partial \tau}{\partial t}\dfrac{\partial}{\partial \tau}+\dfrac{\partial \xi}{\partial t}\dfrac{\partial}{\partial \xi}+\dfrac{\partial \eta}{\partial t}\dfrac{\partial}{\partial \eta} \\ \dfrac{\partial}{\partial x}=\dfrac{\partial \tau}{\partial x}\dfrac{\partial}{\partial \tau}+\dfrac{\partial \xi}{\partial x}\dfrac{\partial}{\partial \xi}+\dfrac{\partial \eta}{\partial x}\dfrac{\partial}{\partial \eta} \\ \dfrac{\partial}{\partial y}=\dfrac{\partial \tau}{\partial y}\dfrac{\partial}{\partial \tau}+\dfrac{\partial \xi}{\partial y}\dfrac{\partial}{\partial \xi}+\dfrac{\partial \eta}{\partial y}\dfrac{\partial}{\partial \eta} \end{cases} \tag{4}$$

or,

$$\begin{pmatrix} \dfrac{\partial}{\partial t} \\ \dfrac{\partial}{\partial x} \\ \dfrac{\partial}{\partial y} \end{pmatrix} = \begin{pmatrix} \tau_t & \xi_t & \eta_t \\ \tau_x & \xi_x & \eta_x \\ \tau_y & \xi_y & \eta_y \end{pmatrix} \begin{pmatrix} \dfrac{\partial}{\partial \tau} \\ \dfrac{\partial}{\partial \xi} \\ \dfrac{\partial}{\partial \eta} \end{pmatrix} \tag{5}$$

where,

$$\tau_t=\frac{\partial \tau}{\partial t} \quad \tau_x=\frac{\partial \tau}{\partial x} \quad \tau_y=\frac{\partial \tau}{\partial y} \tag{6}$$

$$\xi_t=\frac{\partial \xi}{\partial t} \quad \xi_x=\frac{\partial \xi}{\partial x} \quad \xi_y=\frac{\partial \xi}{\partial y} \tag{7}$$

$$\eta_t=\frac{\partial \eta}{\partial t} \quad \eta_x=\frac{\partial \eta}{\partial x} \quad \eta_y=\frac{\partial \eta}{\partial y} \tag{8}$$

Velocity components are transformed as follows:

$$u^\xi = \xi_x u+\xi_y v \tag{9}$$

$$u^\eta = \eta_x u+\eta_y v \tag{10}$$

or,

$$\begin{pmatrix} u^\xi \\ u^\eta \end{pmatrix} = \begin{pmatrix} \xi_x & \xi_y \\ \eta_x & \eta_y \end{pmatrix} \begin{pmatrix} u \\ v \end{pmatrix} \tag{11}$$

$$\begin{pmatrix} u \\ v \end{pmatrix} = \frac{1}{J}\begin{pmatrix} \eta_y & -\xi_y \\ -\eta_x & \xi_x \end{pmatrix} \begin{pmatrix} u^\xi \\ u^\eta \end{pmatrix} \tag{12}$$

where u^ξ and u^η are contravariant components of flow velocity in the ξ- and η- directions. J is the Jacobian of the coordinate transformation, which can be written as follows:

$$\begin{aligned} J = {} & \tau_t\xi_x\eta_y+\xi_t\eta_x\tau_y+\eta_t\tau_x\xi_y \\ & -\eta_t\xi_x\tau_y-\xi_t\tau_x\eta_y-\tau_t\xi_y\eta_x \end{aligned} \tag{13}$$

Using these relations, the basic equations of flow in the MBFC system are given as follows:

$$\frac{\partial}{\partial \tau}\left(\frac{h}{J}\right)+\frac{\partial}{\partial \xi}\left[\left(\xi_t+u^\xi\right)\frac{h}{J}\right]+\frac{\partial}{\partial \eta}\left[\left(\eta_t+u^\eta\right)\frac{h}{J}\right]=0 \tag{14}$$

$$\begin{aligned} & \frac{\partial u^\xi}{\partial \tau}+\left(\xi_t+u^\xi\right)\frac{\partial u^\xi}{\partial \xi}+\left(\eta_t+u^\eta\right)\frac{\partial u^\xi}{\partial \eta} \\ & \quad +\alpha_1 u^\xi u^\xi+\alpha_2 u^\xi u^\eta+\alpha_3 u^\eta u^\eta-D_\xi \\ & =-g\left[\left({\xi_x}^2+{\xi_y}^2\right)\frac{\partial H}{\partial \xi}\left(\xi_x\eta_x+\xi_y\eta_y\right)\frac{\partial H}{\partial \eta}\right] \\ & -\frac{C_d u^\xi}{hJ}\sqrt{\left(\eta_y u^\xi-\xi_y u^\eta\right)^2+\left(-\eta_x u^\xi-\xi_x u^\eta\right)^2} \end{aligned} \tag{15}$$

$$\frac{\partial u^\eta}{\partial \tau}+\left(\xi_t+u^\xi\right)\frac{\partial u^\eta}{\partial \xi}+\left(\eta_t+u^\eta\right)\frac{\partial u^\eta}{\partial \eta}$$

$$+\alpha_4 u^\xi u^\xi + \alpha_5 u^\xi u^\eta + \alpha_6 u^\eta u^\eta - D_\eta$$

$$= -g\left[\left({\eta_x}^2 + {\eta_y}^2\right)\frac{\partial H}{\partial \eta}\left(\xi_x\eta_x + \xi_y\eta_y\right)\frac{\partial H}{\partial \xi}\right]$$

$$-\frac{C_d u^\eta}{hJ}\sqrt{\left(\eta_y u^\xi - \xi_y u^\eta\right)^2 + \left(-\eta_x u^\xi - \xi_x u^\eta\right)^2} \quad (16)$$

where ξ and η are spatial and $\tau(=t$ in the present model) is time coordinates in MBFC system. D_ξ and D_η are momentum diffusion terms in $\xi-$ and $\eta-$ directions, respectively, which are described in Shimizu & Itakura (1991). Coeficients $\alpha_1 \sim \alpha_6$ are given as follows:

$$\alpha_1 = \xi_x\frac{\partial^2 x}{\partial \xi^2} + \xi_y\frac{\partial^2 y}{\partial \xi^2} \quad (17)$$

$$\alpha_2 = 2\left(\xi_x\frac{\partial^2 x}{\partial \xi \partial \eta} + \xi_y\frac{\partial^2 y}{\partial \xi \partial \eta}\right) \quad (18)$$

$$\alpha_3 = \xi_x\frac{\partial^2 x}{\partial \eta^2} + \xi_y\frac{\partial^2 y}{\partial \eta^2} \quad (19)$$

$$\alpha_4 = \eta_x\frac{\partial^2 x}{\partial \xi^2} + \eta_y\frac{\partial^2 y}{\partial \xi^2} \quad (20)$$

$$\alpha_5 = 2\left(\eta_x\frac{\partial^2 x}{\partial \xi \partial \eta} + \eta_y\frac{\partial^2 y}{\partial \xi \partial \eta}\right) \quad (21)$$

$$\alpha_6 = \eta_x\frac{\partial^2 x}{\partial \eta^2} + \eta_y\frac{\partial^2 y}{\partial \eta^2} \quad (22)$$

3 SEDIMENT TRANSPORT EQUATIONS

The continuity equation of two-dimensional bedload transport in MBFC is represented by the following equation:

$$\frac{\partial}{\partial t}\left(\frac{z_b}{J}\right) + \frac{1}{1-\lambda}\left[\frac{\partial}{\partial \xi}\left(\frac{q^\xi}{J}\right) + \frac{\partial}{\partial \eta}\left(\frac{q^\eta}{J}\right)\right] = 0 \quad (23)$$

where z_b is bed elevation, λ is porosity of bed material, and q^ξ and q^η are the contravariant components of the bedload transport rate per unit width in the ξ- and η- directions, which are expressed by assigning s to the direction of the streamline and n to the direction perpendicular to the streamline:

$$q^\xi = \frac{\partial \xi}{\partial s}q^s + \frac{\partial \xi}{\partial n}q^n = \left(\xi_x\frac{\partial x}{\partial s} + \xi_y\frac{\partial y}{\partial s}\right)q^s + \left(\xi_x\frac{\partial x}{\partial n} + \xi_y\frac{\partial y}{\partial n}\right)q^n \quad (24)$$

$$q^\eta = \frac{\partial \eta}{\partial s}q^s + \frac{\partial \eta}{\partial n}q^n = \left(\eta_x\frac{\partial x}{\partial s} + \eta_y\frac{\partial y}{\partial s}\right)q^s + \left(\eta_x\frac{\partial x}{\partial n} + \eta_y\frac{\partial y}{\partial n}\right)q^n \quad (25)$$

where q^s and q^n are the bedload transport rate components in $s-$ and $n-$directions, respectively. The following equation proposed by Hasgawa (2000) is employed for the calculation of q^s.

$$q^s = \frac{17}{\cos\theta_b}\tau_*^{3/2}\left(1 - \frac{\tau_{*c}}{\tau_*}\right)\left[1 - \sqrt{\frac{2\tau_{*c}\cos\theta_b}{\tau_*}} + 2\left(\tan\theta_b - \frac{\partial z_b}{\partial s}\right)\right]\sqrt{\left(\frac{\rho_s}{\rho - 1}\right)dg^3} \quad (26)$$

where θ_b is channel reference slope in downstream direction, ρ_s is density of bed material, d is grain size of bed material, τ_* is non-dimensional bed shear stress, and τ_{*c} is critical non-dimensional bed shear stress obtained by using Iwagaki's equation. Equation 26 is based on Ashida & Michiue's (1972) formula and modified to take into account for the gravitational effect as proposed by Kovacs & Parker(1994).

q^n is given by the following formula proposed by Hasegawa (1984).

$$q^n = q^s\left(\frac{h}{r_s}N_* - \sqrt{\frac{2\tau_{*c}\cos\theta_b}{\tau_*}}\frac{\partial z_b}{\partial n}\right) \quad (27)$$

where r_s is the radius of curvature of a streamline, N_* is the coefficient of strength of secondary flow, μ_s is the static friction coefficient of sand grain, μ_k is the kinetic friction coefficient of sand grain. In the analysis, a constant of N_*= 7.0 given by Engelund (1974) is used, while μ_s and μ_k are set to 1.0 and 0.45, considering the properties of sand.

The first term of the right hand side of Equation 27 represents the intensity of secondary flow in response to the curvature of the stream line. The curvature of stream line is determined by the angle between the stream line ($s-$direction) and x-axis.

$$\frac{1}{r_s} = \frac{\partial \theta_s}{\partial s} = \frac{\partial}{\partial s}\left[\tan^{-1}\left(\frac{v}{u}\right)\right] = \frac{\partial}{\partial T}\left[\tan^{-1}(T)\right]\frac{\partial T}{\partial s} = \frac{1}{1+T^2}\frac{\partial T}{\partial s} \quad (28)$$

where θ_s is the angle between $x-$ and $s-$axis, $T = v/u$, and,

$$\frac{1}{1+T^2} = \frac{1}{1+\left(\frac{v}{u}\right)^2} = \frac{u^2}{u^2+v^2} = \frac{u^2}{V^2} \quad (29)$$

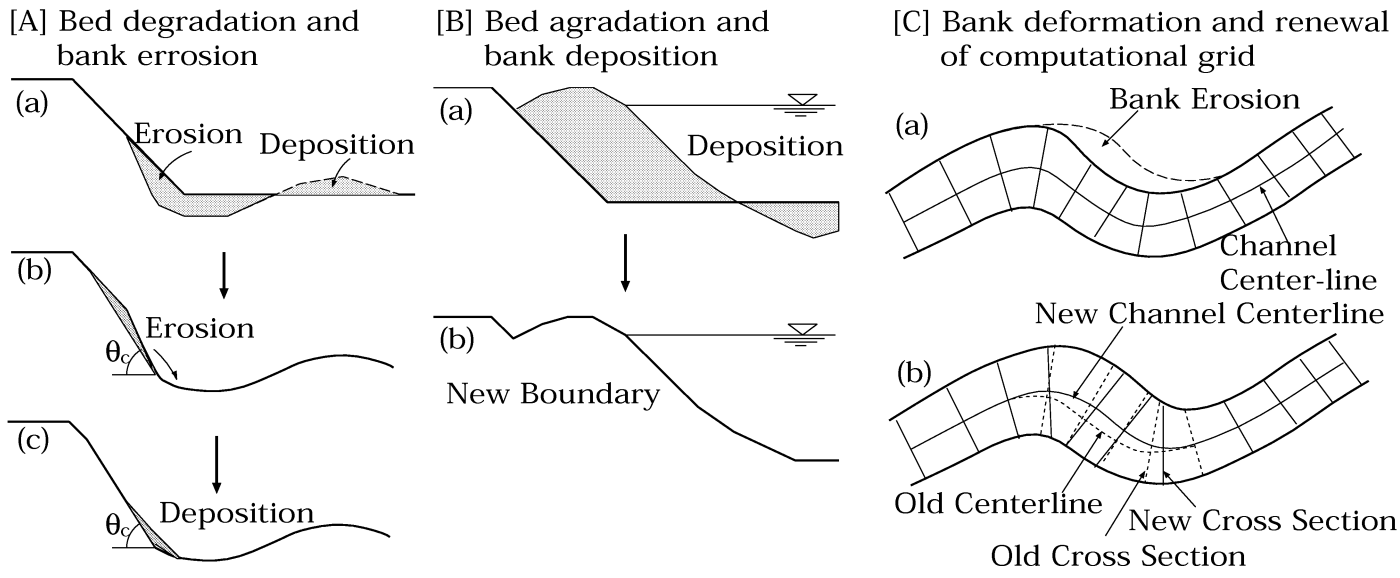

Figure 1. Bed deformation and renewal of channel geometry

$$\frac{\partial T}{\partial s} = \frac{\partial}{\partial s}\left(\frac{v}{u}\right) = \frac{u\dfrac{\partial v}{\partial s} - v\dfrac{\partial u}{\partial s}}{u^2} \tag{30}$$

$$\frac{\partial}{\partial s} = \frac{\partial x}{\partial s}\frac{\partial}{\partial x} + \frac{\partial y}{\partial s}\frac{\partial}{\partial y} = \frac{u}{V}\frac{\partial}{\partial x} + \frac{v}{V}\frac{\partial}{\partial y}$$

$$= \frac{u}{V}\left(\xi_x\frac{\partial}{\partial \xi} + \eta_x\frac{\partial}{\partial \eta}\right) + \frac{v}{V}\left(\xi_y\frac{\partial}{\partial \xi} + \eta_y\frac{\partial}{\partial \eta}\right) \tag{31}$$

where $V = \sqrt{u^2 + v^2}$. Consequently, r_s is determined by the following equation.

$$\frac{1}{r_s} = \frac{1}{V^3}\left[u^2\left(\xi_x\frac{\partial v}{\partial \xi} + \eta_x\frac{\partial v}{\partial \eta}\right) + uv\left(\xi_y\frac{\partial v}{\partial \xi} + \eta_y\frac{\partial v}{\partial \eta}\right)\right.$$

$$\left. -uv\left(\xi_x\frac{\partial u}{\partial \xi} + \eta_x\frac{\partial u}{\partial \eta}\right) - v^2\left(\xi_y\frac{\partial u}{\partial \xi} + \eta_y\frac{\partial u}{\partial \eta}\right)\right] \tag{32}$$

Channel bed slope in $s-$ and $n-$directions, $\partial z_b/\partial s$ and $\partial z_b/\partial n$ used in Eqs. 26 and 27, respectively, are expressed as follows:

$$\frac{\partial z_b}{\partial s} = \frac{\partial z_b}{\partial \xi}\frac{\partial \xi}{\partial s} + \frac{\partial z_b}{\partial \eta}\frac{\partial \eta}{\partial s} =$$

$$\frac{\partial z_b}{\partial \xi}\left(\xi_x\frac{\partial x}{\partial s} + \xi_y\frac{\partial y}{\partial s}\right) + \frac{\partial z_b}{\partial \eta}\left(\eta_x\frac{\partial x}{\partial s} + \eta_y\frac{\partial y}{\partial s}\right) \tag{33}$$

$$\frac{\partial z_b}{\partial n} = \frac{\partial z_b}{\partial \xi}\frac{\partial \xi}{\partial n} + \frac{\partial z_b}{\partial \eta}\frac{\partial \eta}{\partial n} =$$

$$\frac{\partial z_b}{\partial \xi}\left(\xi_x\frac{\partial x}{\partial n} + \xi_y\frac{\partial y}{\partial n}\right) + \frac{\partial z_b}{\partial \eta}\left(\eta_x\frac{\partial x}{\partial n} + \eta_y\frac{\partial y}{\partial n}\right) \tag{34}$$

Non-dimensional bed shear stress, τ_*, in Eqations 26 and 27 is given by:

$$\tau_* = \frac{C_d V^2}{\left(\dfrac{\rho_s}{\rho - 1}\right)gd} = \frac{C_d(u^2 + v^2)}{\left(\dfrac{\rho_s}{\rho - 1}\right)gd} \tag{35}$$

$\partial x/\partial s$, $\partial x/\partial n$, $\partial y/\partial s$ and $\partial y/\partial n$ in Equations 24, 25, 26 and 27 are given by:

$$\frac{\partial x}{\partial s} = \frac{u}{V} = \cos\theta_s, \qquad \frac{\partial y}{\partial s} = \frac{v}{V} = \sin\theta_s \tag{36}$$

$$\frac{\partial x}{\partial n} = -\frac{v}{V} = -\sin\theta_s, \quad \frac{\partial y}{\partial n} = \frac{u}{V} = \cos\theta_s \tag{37}$$

4 BANK EROSION AND CHANNEL MIGRATION

A ξ-axis is drawn along the channel for the given initial plane shape of the channel, and a η-axis is drawn to intersect with the ξ-axis. Then the plane (ξ, η) is properly divided into the parts to make the initial grids for the computations. The computations for the flow and the bed evolution are conducted using the equations described in the previous two sections. With special attention on the bed evolutions near the banks, the deformation in the plane shape of the channel are calculated according to the following procedure.

When computations show that the riverbed near the banks decreases in height as well as the cross-sectional gradient of the bank slope becomes steeper than the submerged angle of repose (θ_c), the sediment beyond the submerged angle

of repose is assumed to be momentarily eroded to the point of this submerged angle of repose [Hasegawa (1983)]. Furthermore, it is assumed that the sediment load equal to the amount of sediment beyond submerged angle of repose, is deposited at the foot of the bank slope (Figure 1[A]). At this time, if the erosion of the bank slope face advances toward the top of the slope, the computational range is enlarged in the cross-sectional direction of the channel. Moreover, if part of the bed near the banks is transformed into land, narrowing the water channel, the computational range is moved to the new waterline (Figure 1[B]). When the computational range is enlarged, for example, due to the erosion of the banks (Figure 1[C](a)), (Figure 1[C](b)), (1) a new central line of the channel passing through the center of new banklines is set. (2) Along this new central line of the channel, new cross-sections perpendicular to this line are set at equal intervals as the initial condition in the ψ- direction. (3) Each cross-section is divided into the grid numbers in the ξ-direction. Thus, new computational meshes are formed, and the computational data are all transformed from old to new computational grid. While transforming all the computational data between the new and old grid, a linear transformation based on geometric locations must be carried out. These calculations are conducted at intervals of a infinitesimal time (Δt) and are continued up to designated time. Note that the values of ξ_t and η_t are calculated through these processes and fed back to the Equations 14, 15 and 16.

5 NUMERICAL MODEL

Flow equations of 14, 15 and 16 are calculated numerically using finite difference method with computational grids in (ξ, η) coordinate system. To solve Equations 15 and 16, a high-order Godunov scheme known as the Cubic Interpolated Psuedo-particle (CIP) method, proposed by Yabe & Ishikawa (1990), is employed. An assumption is made that at very small time increments, the change in time of the velocity components at a point in space can be broken down into the time evolution of the inhomogeneous terms and the time evolution at a point due to the advection of the field. So, in the first step the change in time of the velocity (u^ξ and u^η denoted here as f) is solved as:

$$\frac{\partial f^*}{\partial t} = G \tag{38}$$

where G is the summation of non-advection terms in Equations 15 and 16. Then f is solved in the advection phase as

$$\frac{\partial f}{\partial \tau} + \tilde{u}\frac{\partial f}{\partial \xi} + \tilde{v}\frac{\partial f}{\partial \eta} = 0 \tag{39}$$

where $\tilde{u} = \xi_t + u^\xi$ and $\tilde{v} = \eta_t + u^\eta$. The solution of Equation 39 for small $\Delta\tau$ is simply approximated as:

$$f(\xi, \eta, \tau + \Delta\tau) \approx f(\xi - \tilde{u}\Delta\tau, \eta - \tilde{v}\Delta\tau, \tau) \tag{40}$$

Using the solution of the non-advection phase (Equation 38) this approximation becomes

$$f(\xi, \eta, \tau+\Delta\tau) \approx f^*(\xi-\tilde{u}\Delta\tau, \eta-\tilde{v}\Delta\tau, \tau+\Delta\tau) \tag{41}$$

The trick then is to find the value of f^* at points in space which generally do not lie on the numerical grid points, as specified by the right hand side of Equation 41. If linear interpolation is used to find f^* at points not on the grid, the first order Godunov method is attained. A more accurate solution requires higher order interpolation, and thus high-order Godunov schemes. In the CIP method, a cubic interpolation of f^* is proposed, and when the interpolation is combined with Equation 41 the resultant equation for f at grid point i, j and time $n+1$ is given by:

$$f_{i,j}^{n+1} = \left[(a_1 X + c_1 Y + e_1)X + g_1 Y + f_\xi^*(i,j)\right] X + \left[(b_1 Y + d_1 X + f_1)Y + f_\eta^*(i,j)\right] Y + f^*(i,j) \tag{42}$$

in which,

$$X = -\tilde{u}\Delta\tau, \qquad Y = -\tilde{v}\Delta\tau \tag{43}$$

$$f_\xi^* = \frac{\partial f^*}{\partial \xi}, \qquad f_\eta^* = \frac{\partial f^*}{\partial \eta} \tag{44}$$

$$a_1 = \left\{\left[f_\xi^*(i+1,j) + f_\xi^*(i,j)\right]\Delta\xi + 2\left[f^*(i,j) - f^*(i+1,j)\right]\right\} / \left(\Delta\xi^3\right) \tag{45}$$

$$b_1 = \left\{\left[f_y^*(i,j+1) + f_y^*(i,j)\right]\Delta\eta + 2\left[f^*(i,j) - f^*(i,j+1)\right]\right\} / \left(\Delta\eta^3\right) \tag{46}$$

$$c_1 = \{f^*(i,j) - f^*(i,j+1)$$

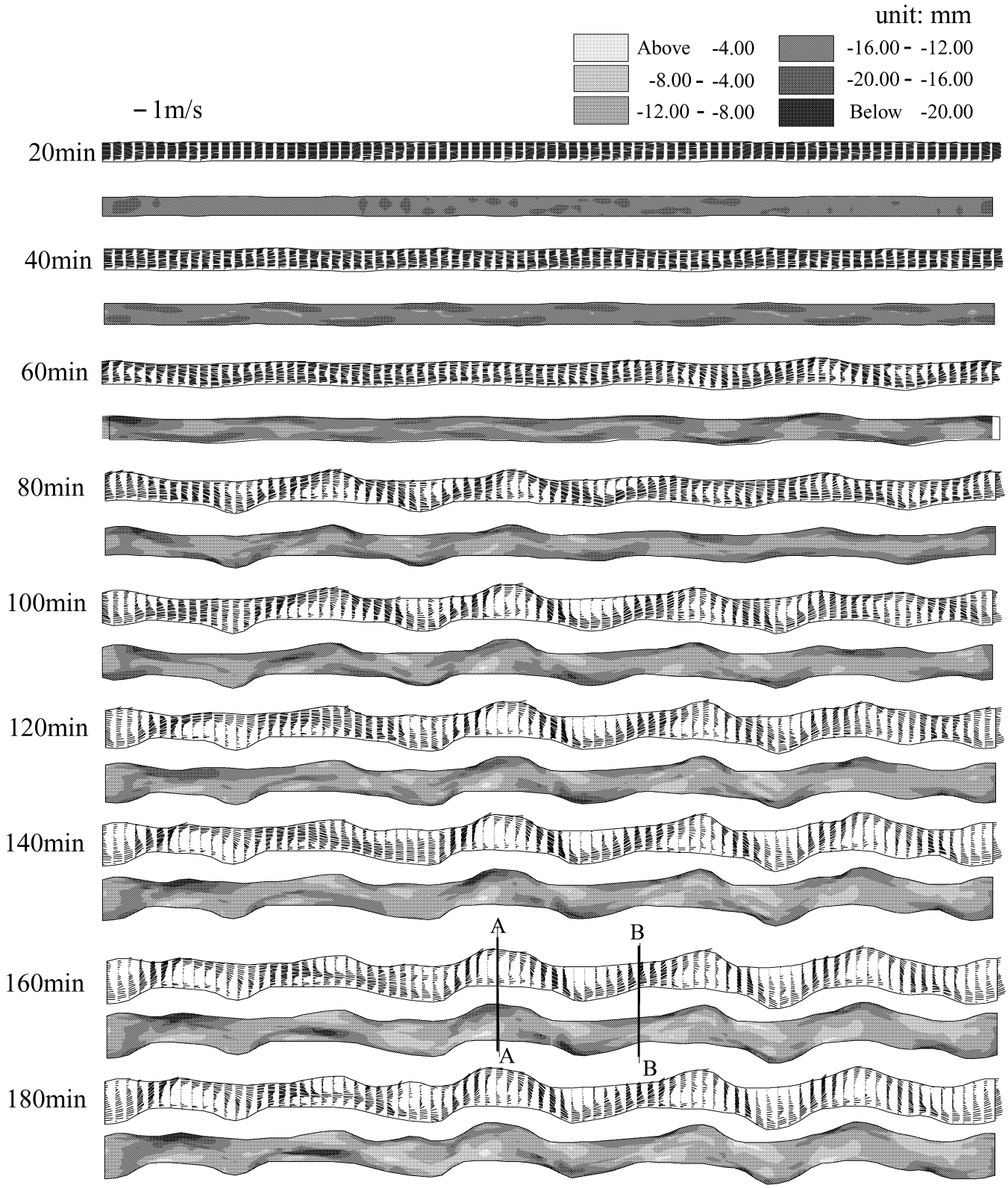

Figure 2. Calculated velocity vector, bed elevation and channel geometry

Table 1: Experimental condition of RUN B1.5-20

Grain Size	d	1.3mm
Slope	S	1.5%
Water Discharge	Q	0.333 $\times 10^{-3}$ m^3/s
Sediment Discharge	Q_s	0.583 g/s

$$-f^*(i+1,j) \quad + \quad f^*(i+1,j+1)$$
$$-\left[f^*_\xi(i,j+1) - f^*_\xi(i,j)\right]\Delta\xi\Big\} / \left(\Delta\xi^2\Delta\eta\right) \quad (47)$$

$$d_1 \quad = \quad \{f^*(i,j) - f^*(i,j+1)$$
$$-f^*(i+1,j) \quad + \quad f^*(i+1,j+1)$$
$$-\left[f^*_\eta(i+1,j) - f^*_\eta(i,j)\right]\Delta\eta\Big\} / \left(\Delta\xi\Delta\eta^2\right) \quad (48)$$

$$e_1 \quad = \quad \{3\left[f^*(i+1,j) - f^*(i,j)\right]$$
$$-\left[f^*_\xi(i+1,j) + 2f^*_\xi(i,j)\right]\Delta\xi\Big\} / \Delta\xi^2 \quad (49)$$

$$f_1 \quad = \quad \{3\left[f^*(i,j+1) - f^*(i,j)\right]$$
$$-\left[f^*_\eta(i,j+1) + 2f^*_\eta(i,j)\right]\Delta\eta\Big\} / \Delta\eta^2 \quad (50)$$

$$g_1 = \left[-f^*_\eta(i+1,j) + f^*_\eta(i,j) - c_1\Delta\xi^2\right] / \Delta\xi \quad (51)$$

In the above instance, it is assumed that $\widetilde{u}$ and $\widetilde{v}$ are negative, so that the advection to the grid points i, j is from within the area, whose vertices are (i,j), $(i{+}1,j)$, $(i,j{+}1)$ and $(i{+}1,j{+}1)$. When $\widetilde{u} \geq 0$ the index $i{+}1$ in Equations 45-51 should be changed to $i-1$, and in tern $\Delta\xi$ becomes $-\Delta\xi$. Similarly, when $\widetilde{v} \geq 0$, $j+1$ and $\Delta\eta$ becomes $j-1$ and $-\Delta\eta$. In the non-advection phase, f^* is calculated from the continuity equation by taking the divergence of the momentum equations and solving for depth as a Poisson equation. The viscous terms are approximated using central differences. Each velocity component is defined in the center of two faces of the computational cells, and depth is defined at the center of the cell. The general procedure, then, is to calculate f^* from Equation 38 in which the convective acceleration terms do not appear. In the second phase f is calculated at the grid points from a pure advection of the cubic interpolated field of f^* by Equations 42-51. These two steps complete the calculation of a single time increment, $\Delta\tau$. The CIP method has been shown to solve the problem of boundedness while introducing little numerical diffusion, and algorithm implementation is more straightforward than other high-order upwind schemes.

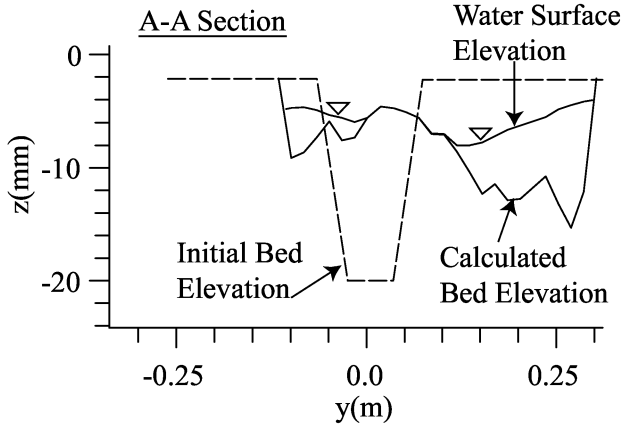

Figure 3: Calculated bed and water surface elevation of section A-A

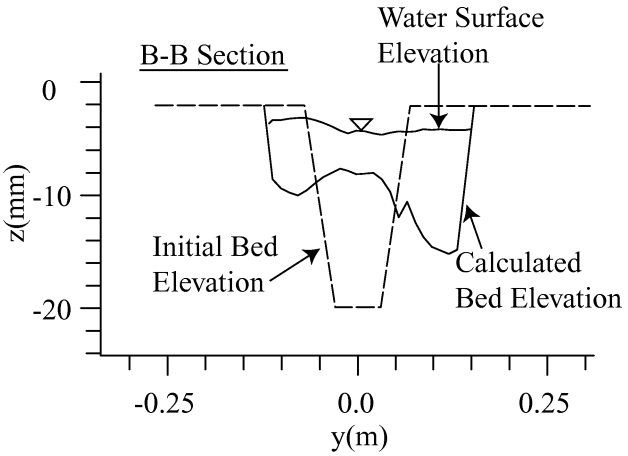

Figure 4: Calculated bed and water surface elevation of section B-B

6 COMPUTATIONAL PROCEDURE

The computational model applies the following process to calculate the changes in flow and the shape of a channel with time at infinitesimal intervals up to the designated time under the given initial conditions.

1. Computing the depth averaged flow field in the given plane shape of a water channel
2. Computing the secondary flow perpendicular to the streamline of the depth averaged flow
3. Computing the sediment transport rate and riverbed evolution
4. The bank erosion, sediment deposition and shape alteration of a channel
5. Setting a coordinate system along a new boundary and updating the computational data
6. Updating time

7 APPLICATION OF THE MODEL

The proposed model is tested with an experimental condition conducted by Bertoldi *et*

al. (2001). The experiment was started with a straight trapezoidal cross section; its base was 0.06m wide and the bank slope was about 40°. During the experiment the evolution of the channel width was continuously monitored by taking pictures along the flume. Bottom topography was surveyed three times of 70, 130 and 150 minutes. Experimental condition of RUN B1.5-20 is summarized in Table 1.

Calculation was conducted under the same condition as the experiment. Figure 2 shows the changes in the bed and the vector of the depth averaged flow velocity with time in the contour map. It is shown that the channel meandering was proceeded while bank erosion was being advanced on right and left bank alternately. From the calculated results, section A-A and B-B at 160 minutes are shown as examples of wide and narrow sections, respectively, in Figures 3 and 4. Figure 3 shows that a mid-channel bar was developed and the channel bifurcation or braiding was observed. Figure 5 shows comparisons between observed and calculated channel geometry and bed elevation at 70, 110 and 150 minutes. The time change of the general geometric characteristics was well reproduced by the proposed model.

8 CONCLUSION

As a first step to develop numerical computation models to simulate the evolution of braided stream with bank erosion, a model to calculate riverbed and riverbanks deformation simultaneously was proposed. A coordinate system was used for the computation in which the boundary can take arbitrary forms. This was because we assumed that erosion and sediment deposition occur laterally, thereby transforming the shape of a channel into arbitrary shapes. The erosion of banks was assumed to occur when the gradient in the cross-sectional direction of the bank becomes steeper than a submerged angle of repose, due to the changes in bed topography near the banks. In this case, the amount of sediment beyond the submerged angle of repose was included in the computation of the riverbed evolution as a supply of sediment from the banks. The model was verified by an experiment on channel widening and braided bar development. As a result, the model was proved to be effective for simulating the changes in braiding accompanying bank erosion. This study confirmed that the model can analyze the braided stream with bank erosion in sandy channel.

REFERENCES

Ashida, K. and Michiue, M. 1972. Study on hydraulic resistance and bed-load transport rate in alluvial streams. *Proc. of JSCE*, No.201, 59–69(in Japanese).

Bertoldi, W., Tubino, M. and Zolezzi, G. 2001. Laboratory measurements on channel bifurcation. *Proc. of 2nd IAHR Symposium on River Coastal and Estuarine Morphodynamics*, 723–732.

Engelund, F. 1974. Flow and bed topography in channel bends. *J. Hyd. Div., ASCE*, 100(11), 1631–1648.

Hasegawa, K., and Ito, H. 1978. Computer simulation of the changing process by year in meandering channel. *Proc. of Hokkaido Chapter of JSCE*, No.32, 197–202(in Japanese).

Hasegawa, K. 1984. Hydraulic research on planimetric forms, bed topographies and flow in alluvial rivers. *Ph. D. Dissertation, Hokkaido Univ., Japan*, 1–184 (in Japanese).

Hasegawa, K. 2000. Hydraulic Characteristics of montain streams and their practical application, *Lecture notes of the 33rd Summer Seminar on Hydrau. Engrg., JSCE*, A-9-1–20(in Japanese).

Kovacs, A. and Parker, G. 1994. A new vectorial bedload formulation and its application to the time evolution of straight river channels. *Jour. of Fluid Mrch.*, 267, 153–183.

Parker, G. 1983. Theory of meander bend deformation, river meandering. *Proc. of Conf. Rivers'83, ASCE.*

Shimizu, Y. and Itakura, T. 1991. Calculation of flow and bed deformation with a general non-orthogonal coordinate system, *Proc. of XXIV IAHR Cong. Madrid, Spain*, Vol. C, 241-248.

Shimizu, Y., Watanabe, Y. and Toyabe, T. 1995. Finite amplitude bed topography in

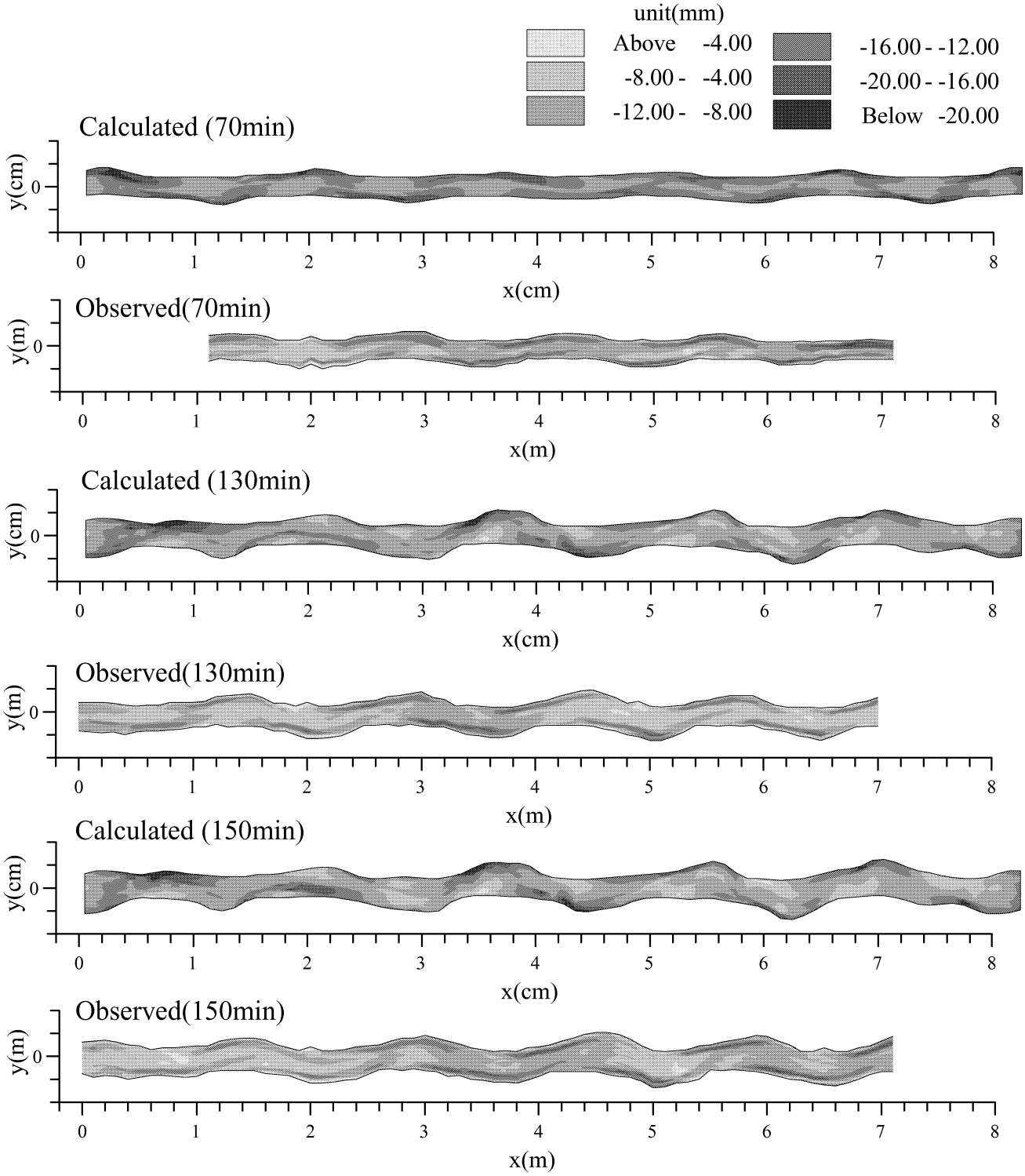

Figure 5. Calculated velocity vector, bed elevation and channel geometry

straight and meandering rivers. *J. Hyd. Coast. and Envir. Engrg., JSCE*, No.509, 67–78(in Japanese).

Yabe, T. and Ishikawa, T. 1990. A numerical cubic-interpolated pseudoparticle (CIP) method without time splitting technique for hyperbolic equations, *Jour. of PSJ*, Vol.59, No.7, 2301–2304.